PNAS RESEARCH ARTICLE | MEDICAL SCIENCES

WASF3 disrupts mitochondrial respiration and may mediate exercise intolerance in myalgic encephalomyelitis/chronic fatigue syndrome

Ping-yuan Wang[a,1], Jin Ma[a,1], Young-Chae Kim[a], Annie Y. Son[a], Abu Mohammad Syed[a], Chengyu Liu[b], Mateus P. Mori[a], Rebecca D. Huffstutler[a], JoEllyn L. Stolinski[c], S. Lalith Talagala[c], Ju-Gyeong Kang[a], Brian T. Walitt[d], Avindra Nath[d], Paul M. Hwang[a,2]

Edited by Se-Jin Lee, University of Connecticut School of Medicine, Farmington, CT; received February 17, 2023; accepted June 27, 2023

Myalgic encephalomyelitis/chronic fatigue syndrome (ME/CFS) is characterized by various disabling symptoms including exercise intolerance and is diagnosed in the absence of a specific cause, making its clinical management challenging. A better understanding of the molecular mechanism underlying this apparent bioenergetic deficiency state may reveal insights for developing targeted treatment strategies. We report that overexpression of *Wiskott-Aldrich Syndrome Protein Family Member 3* (*WASF3*), here identified in a 38-y-old woman suffering from long-standing fatigue and exercise intolerance, can disrupt mitochondrial respiratory supercomplex formation and is associated with endoplasmic reticulum (ER) stress. Increased expression of *WASF3* in transgenic mice markedly decreased their treadmill running capacity with concomitantly impaired respiratory supercomplex assembly and reduced complex IV levels in skeletal muscle mitochondria. WASF3 induction by ER stress using endotoxin, well known to be associated with fatigue in humans, also decreased skeletal muscle complex IV levels in mice, while decreasing WASF3 levels by pharmacologic inhibition of ER stress improved mitochondrial function in the cells of the patient with chronic fatigue. Expanding on our findings, skeletal muscle biopsy samples obtained from a cohort of patients with ME/CFS showed increased WASF3 protein levels and aberrant ER stress activation. In addition to revealing a potential mechanism for the bioenergetic deficiency in ME/CFS, our study may also provide insights into other disorders associated with fatigue such as rheumatic diseases and long COVID.

fatigue | WASF3 | mitochondria | supercomplex | ER stress

Significance

Chronic fatigue is a debilitating symptom that affects many individuals, but its mechanism remains poorly understood. This study shows that endoplamic reticulum (ER) stress–induced WASF3 protein localizes to mitochondria and disrupts respiratory supercomplex assembly, leading to decreased oxygen consumption and exercise endurance. Alleviating ER stress decreases WASF3 and restores mitochondrial function, indicating that WASF3 can impair skeletal muscle bioenergetics and may be targetable for treating fatigue symptoms.

Myalgic encephalomyelitis/chronic fatigue syndrome (ME/CFS), named to reflect its "postinfectious" association, is a debilitating disorder characterized by exercise intolerance estimated to affect ~2.5 million individuals in the U.S. (1, 2). There are no clear abnormalities by clinical testing to explain two prominent physical symptoms of ME/CFS, chronic fatigue and postexertional malaise, thus it is often a diagnosis of exclusion. The physical burdens of this disorder may also be accompanied by cognitive impairment, which further diminishes the patient's quality of life. More recently, chronic fatigue has been associated with the post-COVID-19 syndrome (referred to as "long COVID") and reported to bear resemblance to ME/CFS, raising the possibility that the pathophysiology of these two clinical entities may be related (3).

Although the pathogenesis of ME/CFS has been extensively studied, no specific mediator molecule has been identified to explain the low aerobic capacity in this disorder. A number of ME/CFS studies have revealed redox imbalance and bioenergetic defects, both regulated by the mitochondria (4). Cardiopulmonary exercise testing of individuals with ME/CFS has shown decreased oxygen utilization and increased lactate accumulation, suggesting mitochondrial dysfunction (4–6). An important aspect of oxidative phosphorylation for ATP synthesis is the assembly of mitochondrial respiratory complexes into supercomplexes, which may reduce reactive oxygen species generation by facilitating the efficient transfer of electrons during respiration (7). Studies have shown that supercomplex formation in skeletal muscle is promoted by exercise and is positively correlated with mitochondrial oxygen consumption while metabolic dysfunction is associated with disruption of the supercomplexes (8, 9). During the clinical investigation of a patient with chronic fatigue, we found that WASF3, induced by ER stress, disrupts mitochondrial supercomplex formation and respiration by analyzing an aberrant signaling pathway observed in the patient's cells. Our study provides a molecular explanation for the patient's bioenergetic deficiency, which may be applicable to not only ME/CFS but also other conditions that feature chronic fatigue such as long COVID or rheumatic diseases associated with ER stress (10–12).

Author affiliations: [a]Cardiovascular Branch, National Heart, Lung, and Blood Institute, NIH, Bethesda, MD 20892; [b]Transgenic Core, National Heart, Lung, and Blood Institute, NIH, Bethesda, MD 20892; [c]NIH MRI Research Facility, National Institute of Neurological Disorders and Stroke, NIH, Bethesda, MD 20892; and [d]Clinical Neurosciences Program, National Institute of Neurological Disorders and Stroke, NIH, Bethesda, MD 20892

Author contributions: P.-y.W., J.M., C.L., S.L.T., B.T.W., A.N., and P.M.H. designed research; P.-y.W., J.M., Y.-C.K., A.Y.S., A.M.S., C.L., R.D.H., J.L.S., and J.-G.K. performed research; C.L. contributed new reagents/analytic tools; P.-y.W., J.M., Y.-C.K., C.L., M.P.M., S.L.T., J.-G.K., B.T.W., A.N., and P.M.H. analyzed data; R.D.H. and B.T.W. recruited patients; and P.-y.W. and P.M.H. wrote the paper.

The authors declare no competing interest.

This article is a PNAS Direct Submission.

[1]P.-y.W. and J.M. contributed equally to this work.

[2]To whom correspondence may be addressed. Email: hwangp@mail.nih.gov.

This article contains supporting information online at https://www.pnas.org/lookup/suppl/doi:10.1073/pnas.2302738120/-/DCSupplemental.

Published August 14, 2023.

Results

Decreased Mitochondrial Function in a Patient with Chronic Fatigue. Patient S1 presented as a 38-y-old woman with Li-Fraumeni syndrome (LFS), an early-onset cancer disorder caused by germline mutations of *TP53,* and with a history of worsening fatigue that started after an episode of mononucleosis at age 16. She reported cramps in her lower limb muscles, similar to that associated with strenuous exercise but occurring at rest, and exercise intolerance that required days to recover after physical exertion. Neither her father nor brother, who were also *TP53* mutation carriers, reported chronic fatigue symptoms. Her past medical history was remarkable for the successful treatment of two separate early-onset breast cancers, as well as extensive evaluation of her fatigue symptoms that resulted in the suspected diagnoses of undifferentiated connective tissue disorder, systemic lupus erythematosus, and most recently, Sjogren's syndrome by biomarkers. She was also evaluated for mitochondrial diseases at a tertiary referral center with extensive tests including mitochondrial genomic DNA sequencing and skeletal muscle biopsy studies, all of which were nondiagnostic. Subject S2 is patient S1's 34-y-old male sibling carrying the same *TP53* mutation P152L. He was healthy and did not have any history of cancer or fatigue symptoms. The siblings consented to clinical investigation at the NIH Clinical Research Center.

Measuring the regeneration of phosphocreatine (PCr) after its utilization by exercise in skeletal muscle using ^{31}P-MRS can non-invasively assess mitochondrial ATP synthesis capacity (13). In this test, the subjects perform a brief exercise using their feet while the ^{31}P-PCr spectra of their leg muscle are obtained. The PCr recovery time constant (Tc) is calculated by fitting the postexercise PCr amplitudes to a monoexponential recovery curve. The experiment is repeated after a 25-min rest following the first scan. Using this technique, the PCr Tc in the tibialis anterior muscle of the patient (S1) was found to be markedly prolonged at 80 s compared with reported values of 37 to 40 s in healthy volunteers (Fig. 1*A*) (13, 14). As a control, the PCr Tc of patient's male sibling (S2) carrying the same *TP53* mutation was measured at 30 s, consistent with that of other LFS patients as previously reported (14). To confirm the abnormally slow PCr recovery in patient S1, a follow-up test was conducted several months after measuring control S2. Repeat testing of patient S1 showed that her PCr Tc remained at 80 s, demonstrating the reproducibility of this measurement and the persistence her symptom over time (Fig. 1*A*). The delayed PCr Tc of patient S1 was corroborated by previously published ^{31}P-MRS studies, which also showed slow PCr recovery in the muscle of ME/CFS patients (15).

Paralleling these in vivo findings, the fibroblasts of patient S1 displayed lower OCR (Fig. 1*B*) and decreased respiratory CIV (cytochrome c oxidase) as indicated by subunit MTCO1 and MTCO2 protein levels (Fig. 1*C*) compared with that of her sibling control S2. Because both siblings carried the same *TP53* mutation which can affect mitochondrial function (14), we examined their p53 levels and observed that the p53 of S1 migrated faster than that of S2 in protein gel electrophoresis (Fig. 1*C*). Using a series of antibodies for p53 modifications, the p53 in S1 cells were found to be highly phosphorylated at Ser46 (Fig. 1*C*). Increased phosphoactivation of mitogen-activated protein kinase p38 (MAPK14), which can phosphorylate p53 Ser46, was observed in S1 cells. However, the p38 upstream kinase MKK3 and another MAPK c-Jun N-terminal kinase (JNK), also involved in cell stress response, were not activated in S1 cells, indicating regulation of p38 by a noncanonical pathway (Fig. 1*C*). Intriguingly, it had been reported that the p38 MAPK signaling pathway can also be activated by WASF3, which coincidentally had been implicated as a top candidate gene associated with chronic fatigue syndrome in a large database meta-analysis (16–18). Given the lack of follow-up studies on WASF3 and ME/CFS, we investigated this signaling pathway and observed increased levels of WASF3 protein in patient S1 cells compared with control S2 cells (Fig. 1*C*). Quantification of the data revealed ~40% increase of WASF3 and ~34% decrease of MTCO1 in the patient S1 cells compared to the control S2 cells (Fig. 1 *C*, *Bottom*).

WASF3 Suppresses Mitochondrial Respiration. Demonstrating a causal relationship, knocking down WASF3 in patient S1 cells using shRNA improved basal respiration and significantly boosted spare respiratory capacity (SRC), a robust measure of mitochondrial function, to the level of control S2 cells (Fig. 1*D*). In parallel, reducing WASF3 increased the subunit levels of CIV, but not of the other complexes, while decreasing the phosphorylations of p53 and p38, but not JNK in S1 cells (Fig. 1*E* and *SI Appendix*, Fig. S1). The direct knockdown of p38 also decreased p53 phosphorylation, suggesting that these changes in signaling were downstream effects of increased WASF3 and its inhibition of respiration (*SI Appendix*, Fig. S2). As further confirmation of this signaling pathway, knocking down WASF3 in human myoblasts with or without *TP53* mutation and control human fibroblasts all showed increased mitochondrial SRC and decreased p38 phosphorylation (*SI Appendix*, Fig. S3). In contrast, overexpressing WASF3 in mouse C2C12 myoblasts with wild-type p53 induced p38 phosphorylation while decreasing respiration and subunits of complex IV, but not other complexes (Fig. 2 *A* and *B*). Notably, some subunits of other respiratory complexes were increased by WASF3 overexpression, suggesting that a feedback signal for mitochondrial biogenesis was activated by WASF3 disruption of mitochondria (Fig. 2*A*). Indeed, WASF3 overexpression markedly induced the transcription of mitochondrial biogenesis gene *PGC1α* and some representative respiratory complex genes including *MTCO1* (*SI Appendix*, Fig. S4). In further support of this interpretation, knocking down p38 in the WASF3-overexpressing myoblasts worsened mitochondrial respiration and reduced PGC1α levels (*SI Appendix*, Fig. S5). Collectively, these results showed that primary overexpression of WASF3 in cells leads to the disruption of respiration, which in turn may activate compensatory responses such as p38 phosphorylation for promoting mitochondrial biogenesis. Our findings also suggest that WASF3 posttranslationally regulates mitochondrial complex IV as evidenced by decreased protein but increased mRNA levels of complex IV subunits in cells overexpressing WASF3 (*SI Appendix*, Fig. S4). Furthermore, the regulation of mitochondrial respiration by WASF3 was not found to be restricted to a specific cell type or linked to p53 mutation status.

WASF3 Overexpression Decreases Mouse Exercise Capacity and Mitochondrial Metabolism. The WASF3 amino acid sequence is highly conserved across species, with human WASF3 showing 98% similarity to mouse WASF3, indicating preservation of its function across species. To examine the effect of WASF3 on mitochondrial function and exercise capacity in vivo, we used a human bacterial artificial chromosome (BAC) clone of WASF3 to generate transgenic mice (WASF3 Tg). This approach allowed WASF3 to be expressed under endogenous regulatory control with respect to its levels and tissue specificity. WASF3 Tg mice derived from two different transgenic lines were obtained, and DNA PCR screening showed that they had ~five to six copies of the WASF3 gene present in their genome.

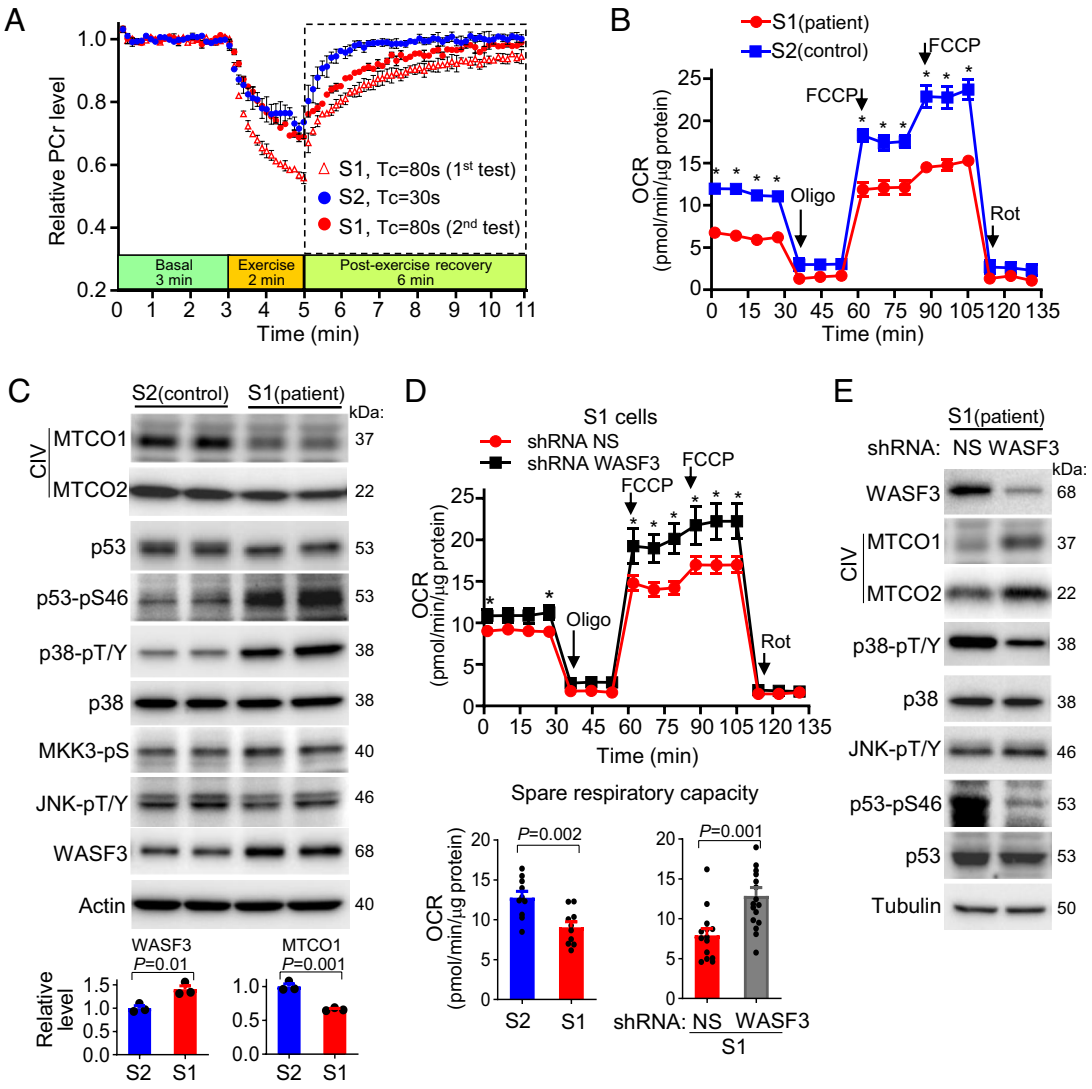

Fig. 1. Mitochondrial dysfunction in a patient with chronic fatigue associates with increased WASF3 expression. (*A*) Noninvasive assessment of in vivo mitochondrial function in a patient with lifelong fatigue (S1) compared with a control sibling (S2) using ^{31}P-MRS. The phosphocreatine (PCr) recovery time constant (T_c) in their tibialis anterior muscle was calculated from PCr levels measured during the recovery phase after foot exercise. The *y* axis shows PCr levels relative to the preexercise baseline (mean and range of two scans are shown). The ^{31}P-MRS test of patient S1 was repeated (2nd test) after control S2 testing was performed. (*B*) Oxygen consumption rate (OCR) of skin fibroblasts obtained from S1 and S2. Specificity of OCR is demonstrated by using complex I (rotenone, Rot) and complex V (oligomycin, Oligo) inhibitors (n = 5). (*C*) Immunoblots of two independently cultured fibroblast samples of siblings S1 and S2. MTCO1 and MTCO2 denote mitochondrial cytochrome c oxidase subunits 1 and 2, respectively, of respiratory complex IV (CIV). pS and pT/Y denote phosphorylated serine and threonine/tyrosine, respectively. Levels of WASF3 and MTCO1 were quantified (n = 3). (*D*) OCR measured in patient S1 fibroblasts after knockdown of WASF3 (n = 7 to 10). Cells were transduced with lentivirus expressing nonspecific (NS) or WASF3 shRNA. Spare respiratory capacities (calculated by subtracting basal OCR from maximal OCR after FCCP treatment) of the cells were also compared as follows: Patient S1 vs. Control S2; NS shRNA vs. WASF3 shRNA transduced S1 cells (n = 14 to 17). (*E*) Immunoblots of S1 fibroblasts after WASF3 knockdown (also refer to *SI Appendix*, Fig. S1) (one representative blot of n = 3). Values are mean ± SE. Statistical difference by unpaired, two-tailed Student's *t* test. *$P < 0.05$.

Examination of various tissues of the transgenic mice revealed significantly increased levels of WASF3 in different skeletal muscle groups (tibialis anterior, gastrocnemius, and soleus) in association with decreases in the subunits of complex IV but not of other respiratory complexes (Fig. 2 *C* and *D* and *SI Appendix*, Figs. S6*A* and S7*A*). In contrast to skeletal muscle, WASF3 levels in the heart, brain, and liver were not as apparently increased, possibly due to tissue-specific variations in the basal expression and regulation of *WASF3* (19, 20), albeit there was evidence of mild reductions in complex IV subunits (Fig. 2*C* and *SI Appendix*, Fig. S6*A*). As observed in WASF3 overexpressing myoblasts, the mRNA levels of mitochondrial genes, such as ND1, MTCO1, and ATP6, were significantly increased in skeletal muscle and heart of the WASF3 Tg mice, likely representing a feedback response to WASF3 disruption of mitochondrial function (*SI Appendix*, Fig. S6*B*).

To measure mitochondrial function in intact skeletal muscle, we selected the soleus muscle as it is predominantly composed of slow-twitch fibers enriched in mitochondria. Furthermore, its small size (~10 mg) makes it amenable to ex vivo measurement of OCR and ECAR as simultaneous measures of oxphos and glycolysis, respectively. WASF3 Tg soleus muscle, with confirmed reciprocal changes in WASF3 and MTCO1/2 levels (*SI Appendix*, Fig. S7*A*), showed significantly lower OCR to ECAR ratio as an index of oxidative metabolism compared with that of wild-type mice, indicating increased WASF3 reprograms its metabolism toward glycolysis (Fig. 2 *E*, *Left*). In support of this, the WASF3 Tg mice showed higher blood lactate levels

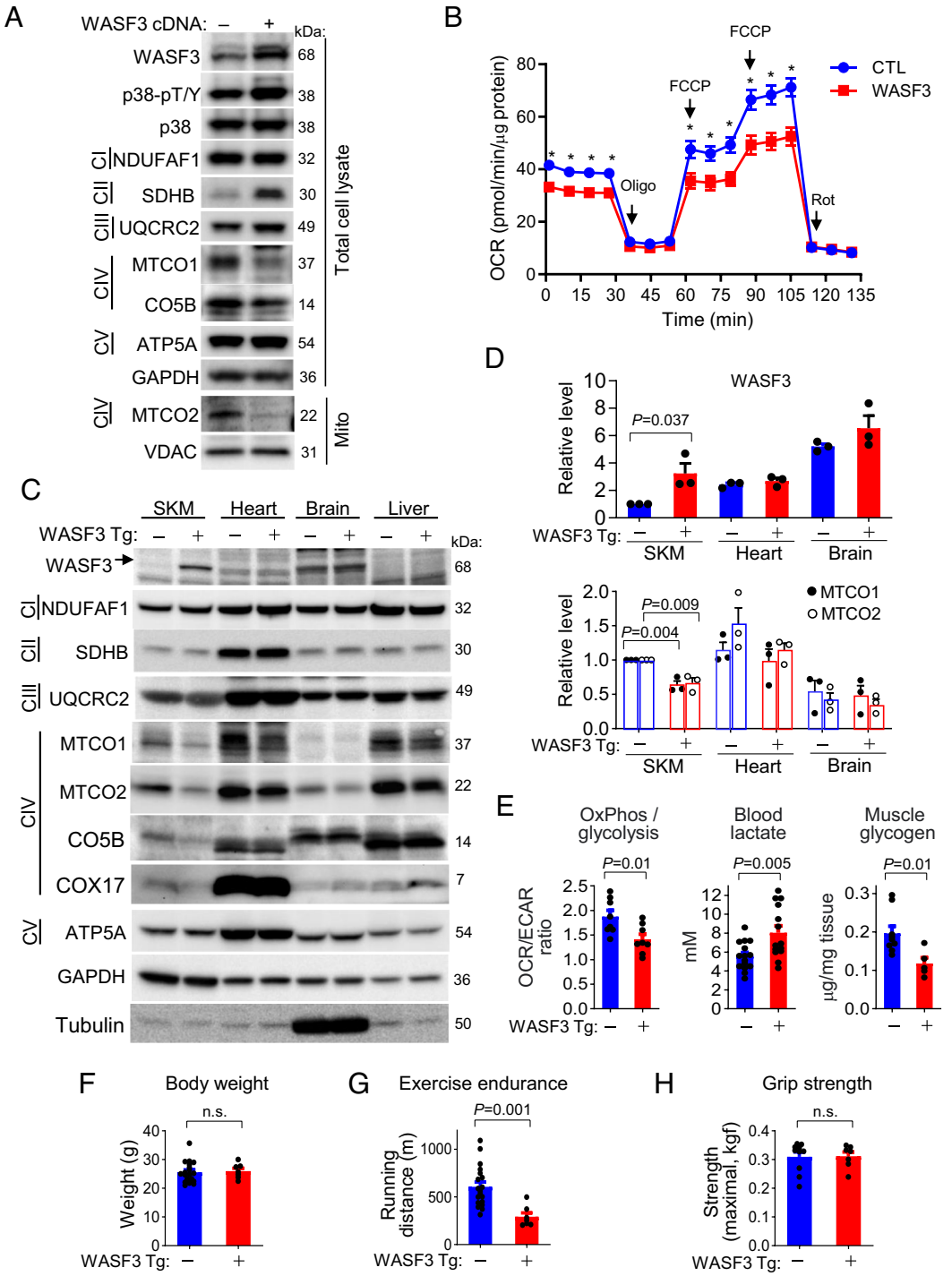

Fig. 2. WASF3 overexpression disrupts mitochondrial respiration and decreases exercise capacity in mice. (*A*) Immunoblots of C2C12 myoblasts stably transfected with empty vector or WASF3 cDNA. Mitochondria (Mito) were purified for immunoblotting MTCO2 in the C2C12 cells (one representative blot of n = 3). (*B*) Oxygen consumption rate (OCR) of C2C12 cells as described in panel *A* (n = 13). (*C*) Immunoblots of WASF3 and other indicated proteins in hindlimb tibialis anterior muscle (SKM) and other tissues of ~10-wk-old WASF3 Tg and wild-type mice (one representative blot of n = 3). (*D*) Levels of WASF3 and MTCO1/2 from immunoblots shown in panel (*C*) were quantified and normalized to that in SKM of wild-type mice (n = 3). (*E*, *Left*) OCR and extracellular acidification rate (ECAR) of whole soleus muscle from ~10-wk-old mice were measured simultaneously using a Seahorse XF24 Analyzer. Shown are ratios of OCR to ECAR, representing oxidative phosphorylation and glycolysis, respectively (n = 8). *Middle* panel: lactate levels in tail blood of ~10-wk-old mice (n = 14 to 15). *Right* panel: glycogen content of gastrocnemius muscles of ~16-wk-old mice (n = 5 to 9). (*F*) Body weights of 10-wk-old WASF3 Tg and littermate wild-type male mice (n = 7 to 19). (*G*) Exercise endurance of 10-wk-old WASF3 Tg compared with littermate wild-type mice measured by treadmill testing (n = 7 to 19). (*H*) Four-paw grip strength of indicated ~13-wk-old mice (n = 7 to 10). Male mice were used for all experiments. Values are mean ± SE. Statistical difference by unpaired, two-tailed Student's *t* test. **P* < 0.05; n.s. (nonsignificant).

compared with that of wild-type mice, reflecting the finding of elevated blood lactate in ME/CFS patients at rest, which correlated with their postexertional malaise severity (Fig. 2 *E*, *Middle*) (21). Moreover, the glycogen levels in the skeletal muscle of WASF3 Tg mice were significantly lower than that of wild-type mice, apparently due to increased glucose utilization secondary to mitochondrial disruption by WASF3 (Fig. 2 *E*, *Right*).

Although the WASF3 Tg mice appeared morphologically similar to their wild-type littermates with no overt differences in behavior or lifespan (>1.5 y), they showed a remarkable ~50% reduction in maximal running capacity by treadmill testing while their paw grip strength did not show a difference from that of wild-type mice (Fig. 2 *F*–*H*). In addition, EM images of longitudinal sections of skeletal muscle did not reveal a significant difference in the striated pattern of myofilaments between WASF3 Tg and wild-type mice (*SI Appendix*, Fig. S7 *B* and *C*). The levels of α-actinin, which anchors actin myofilaments in the sarcomere, were also unchanged (*SI Appendix*, Fig. S7*A*). These results suggested that the disruptive effect of WASF3 on respiration may be more likely to play a role in determining the reduced exercise endurance of the WASF3 Tg mice (Fig. 2*G*) (22).

WASF3 Localizes to Mitochondria and Regulates Respiratory Supercomplex Assembly. We next investigated how WASF3 disrupts mitochondrial respiration. WASF3 has been reported to be associated with the mitochondrial membrane, where the respiratory complexes reside, and to interact with ATAD3A and GRP78 (ER chaperone BiP) at the contact sites of the mitochondria and endoplasmic reticulum (23). Subcellular fractionation of C2C12 myoblasts with or without WASF3 transfection demonstrated its enrichment in the mitochondria (Fig. 3*A*). Interestingly, mitochondrial WASF3 migrated faster (lower band) than the cytosolic form on SDS-PAGE, suggesting a specific posttranslational modification for its subcellular localization (Fig. 3*A*). The empiric treatment of the C2C12 cell lysate with alkaline phosphatase shifted the lower WASF3 band to the upper position, indicating

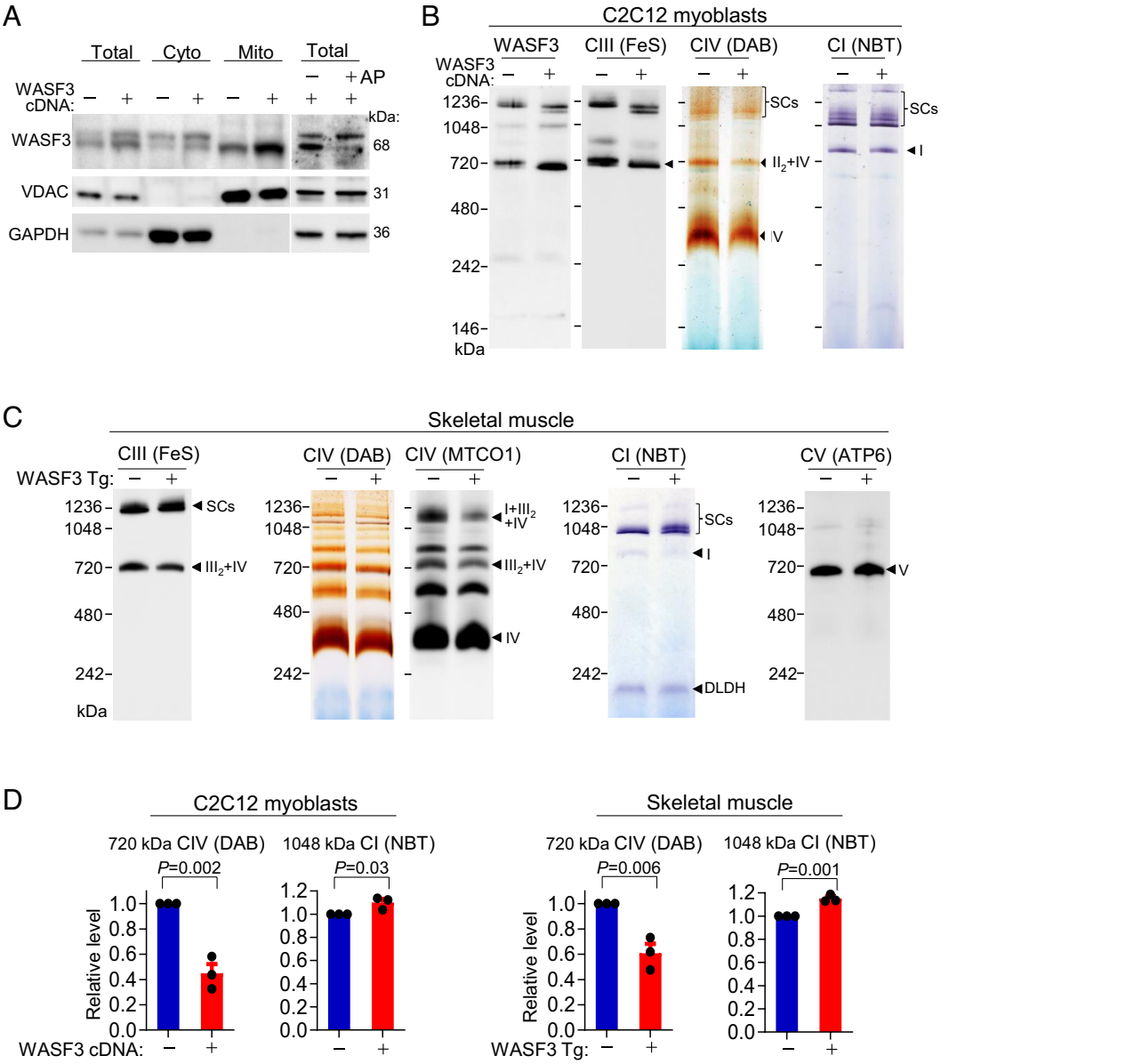

Fig. 3. WASF3 localizes to mitochondria and disrupts respiratory supercomplex formation. (*A*) Immunoblots of the subcellular fractions (10-μg protein per lane) isolated from C2C12 myoblasts expressing control empty (−) or WASF3 cDNA-containing vector (one representative blot of n = 3). Alkaline phosphatase (AP). (*B*) Mitochondria isolated from the C2C12 cells as described in panel *A* were solubilized in 1% digitonin, resolved by BN-PAGE, and then immunoblotted with antibodies against WASF3 and CIII Rieske FeS protein (UQCRFS1). The corresponding positions of respiratory complexes CI and CIV were visualized by in-gel enzymatic assays using nitroblue tetrazolium (NBT) and diaminobenzidine (DAB), respectively (one representative blot or in-gel activity assay of n = 3). (*C*) Mitochondria from wild-type (−) or WASF3 Tg mouse hindlimb gastrocnemius muscle were resolved by BN-PAGE and immunoblotted using the indicated antibodies. In-gel activities of CI and CIV were visualized to confirm the supercomplexes detected by immunoblotting. Immunoblot of CV subunit ATP6 serves as control. Protein MW markers in kDa (one representative blot or in-gel activity assay of n = 3). (*D*) In-gel activity bands of CIV (DAB-stained, 720 kDa) and CI (NBT-stained, 1,048 kDa) were quantified (n = 3). Values are mean ± SE. Statistical difference by unpaired, two-tailed Student's *t* test.

that WASF3 in mitochondria may be phosphorylated (Fig. 3 *A*, *Right* 2 lanes).

WASF3 is known to play an important role in regulating cytoskeletal actin dynamics by acting as a scaffold for signaling protein complexes, so we wondered whether it may interact with respiratory complexes of mitochondria (24). Blue native polyacrylamide gel electrophoresis (BN-PAGE) enables the separation of different supercomplexes composed of respiratory complexes with defined stoichiometry (7). WASF3 immunoblotting after BN-PAGE of mitochondrial lysates isolated from C2C12 myoblasts transfected with WASF3 cDNA revealed a specific increase in the immunoreactivity of a ~720-kDa band, suggesting that WASF3 associates with the respiratory supercomplex (SC) III_2+IV (Fig. 3 *B*, *Left*) (25). Notably, there were concomitant decreases in the intensity of the 720-kDa band when immunoblotted by antibody against the CIII subunit Rieske iron-sulfur (FeS) redox protein (UQCRFS1) or by in-gel CIV cytochrome c oxidase (COX) activity (DAB staining), while the intensity of bands corresponding to CI activity (NBT staining) in the same samples was not reduced (Fig. 3*B* and *SI Appendix*, Fig. S8*A*). Similar results were observed in the mitochondria of myotubes derived from the myoblasts (*SI Appendix*, Fig. S8*B*). Consistent with the results of WASF3-overexpressing C2C12 myoblasts and myotubes, skeletal muscle mitochondria of WASF3 Tg mice also showed reduced levels of SC III_2+IV as detected by FeS protein and MTCO1 antibodies or in-gel assay of CIV activity (Fig. 3*C* and *SI Appendix*, Fig. S8*C*). Again as controls, the levels of CI activity and ATP6 (a subunit of CV) were not decreased in mitochondria from WASF3 Tg mice (Fig. 3 *C*, *Right*). Quantification of the SC III_2+IV in-gel COX activity revealed ~50% reductions in WASF3 Tg mouse and WASF3-transfected cells, while their CI activity appeared even higher than that in their respective controls (Fig. 3*D*). Together, these data showed that increased WASF3 disrupted the stoichiometry of mitochondrial respiratory complexes. The levels of WASF3 were not found to be significantly increased in the hearts of WASF3 Tg mice (Fig. 2 *C* and *D*), and as a result, there were no observable alterations in their stoichiometry of mitochondrial respiratory complexes or overall mitochondrial activity (*SI Appendix*, Fig. S9).

WASF3 Interacts with Mitochondrial Complex III and Prevents Supercomplex $CIII_2$+IV Formation. CIII is the center of the respiratory chain and normally exists as a dimer (III_2), which can recruit CIV to form SC III_2+IV (26, 27). To test whether WASF3 is physically involved in supercomplex assembly, the mitochondrial lysate was preincubated with nonimmune IgG or WASF3 antibody and then resolved by BN-PAGE. The WASF3 antibody more selectively reduced the SC III_2+IV band at 720 kDa while showing no significant effect on CI band as assessed by NBT activity in either control or WASF3-overexpressing samples (Fig. 4*A* and *SI Appendix*, Fig. S10). These results indicate that SC III_2+IV contains the WASF3 protein and that the antibody binding, similar to an increase in WASF3 protein level, may cause interference and disrupt supercomplex formation (Fig. 4*A*).

To further demonstrate that WASF3 interacts with respiratory supercomplexes, a proximity-dependent biotinylation assay using chimeric WASF3-biotin ligase (BirA) was performed. It has been reported that the N terminus of WASF3 is embedded in mitochondrial membrane while its C-terminal end interacts with actin (23). Therefore, to assess its mitochondrial role, full-length WASF3 (amino acid residues 1-499)-BirA-HA, C-terminal truncated WASF3 (amino acid residues 1-332)-BirA-HA, or control BirA-HA was transiently expressed in C2C12 myoblasts.

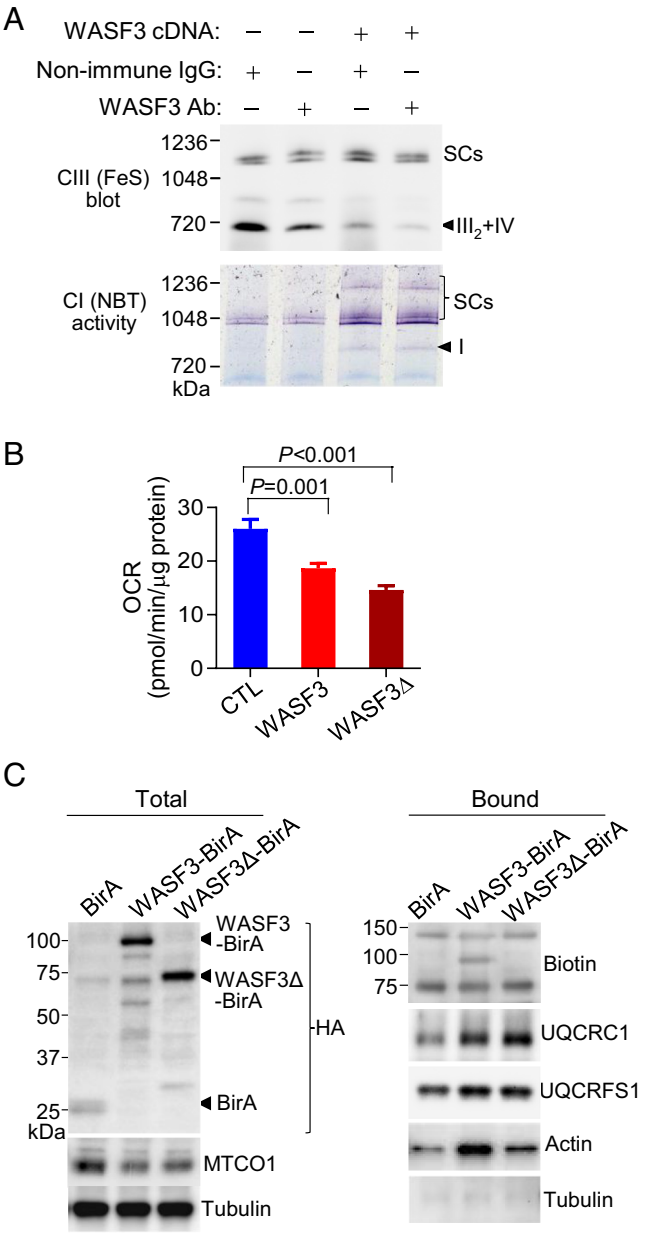

Fig. 4. WASF3 interacts with mitochondrial CIII and prevents supercomplex $CIII_2$+IV formation. (*A*) Mitochondrial lysates of C2C12 myoblasts with or without WASF3 cDNA expression were incubated with control IgG or WASF3 antibody, resolved by BN-PAGE, and immunoblotted with CIII Rieske FeS protein antibody. The upper band at ~1,048 kDa serves as an internal control for the decreased SC III_2+IV band. CI in-gel activity was also visualized by NBT (one representative blot or in-gel activity assay of n = 3). (*B*) Transient expression (48 h) of empty-vector control (CTL), full-length WASF3 (amino acid residues 1-499), or C terminus truncated WASF3 (WASF3Δ, amino acid residues 1-332) in C2C12 cells and its effect on mitochondrial OCR (n = 6 to 7, two experimental repeats). (*C*) Plasmid vector containing HA-tagged biotin ligase (BirA), or the BirA-fused to the C terminus of full-length or C terminus truncated (WASF3Δ) WASF3 was transiently transfected into C2C12 myoblasts for 24 h. Total cell lysates were immunoblotted for the HA-tagged BirA or its chimeric proteins and MTCO1. The right panel shows biotinylated proteins bound to streptavidin beads immunoblotted with the indicated antibodies. Actin, known to interact with the C terminus of WASF3, and tubulin serve as specificity controls for the interaction assay. Protein MW markers in kDa. Values are mean ± SE. Statistical difference by one-way ANOVA.

Overexpression of either the full-length or truncated WASF3 inhibited mitochondrial respiration and decreased MTCO1 levels as predicted (Fig. 4 *B* and *C*, *Left*). Although there was similar nonspecific biotinylation by all 3 constructs (Fig. 4*C*, *Right* panel labeled "Biotin"), both the full-length and truncated WASF3

specifically increased the biotinylation of the CIII subunit Core I protein 1(UQCRC1) and Rieske FeS redox protein (UQCRFS1), which are known to be important for CIII assembly and dimeric III_2 stability, respectively (Fig. 4 *C*, *Right*) (26). As a specificity control, the full length, but not the C-terminal truncated, WASF3-BirA promoted the biotinylation of actin while tubulin and MTCO1 were largely undetectable in the streptavidin-bound fraction (Fig. 4*C*). These results favored a model in which WASF3 is in close proximity to CIII and may interact with the complex via its N-terminal part to prevent the formation of SC III_2+IV. Taken together, these data showed that overexpressed WASF3 can interfere with mitochondrial supercomplex formation and cause CIV deficiency via protein–protein interaction, thereby decreasing mitochondrial respiration.

WASF3 is Overexpressed in Skeletal Muscle of ME/CFS Patients and is Associated with ER Stress. A number of studies over the years have suggested that acquired mitochondrial dysfunction underlies the symptoms of ME/CFS (4, 28, 29). Given the typical ME/CFS clinical features of exercise intolerance and postexertional malaise exhibited by patient S1, we wondered whether altered levels of WASF3 may also contribute to bioenergetic deficiency in this disorder. Immunoblotting of deidentified skeletal muscle biopsy samples obtained from a comprehensive study exploring the clinical and biological phenotypes of postinfectious ME/CFS patients revealed significantly increased WASF3 levels with concomitant decreases in CIV subunit proteins compared with healthy volunteers (Fig. 5 *A* and *B* and *SI Appendix*, Fig. S11) (ClinicalTrials.gov NCT02669212) (30). This interesting association raised the question of how WASF3 expression might be regulated and potentially contribute to the bioenergetic deficiency in this syndrome.

WASF3 has been reported to be regulated by BiP (GRP78), an endoplasmic reticulum (ER) chaperone for protein quality control whose defective response can cause ER stress and metabolic disorders (23, 31). Given the importance of the interaction between the ER and mitochondria for muscle function (32), we reasoned that ER stress, also reported to play a role in rheumatic diseases which often feature fatigue (10), may regulate WASF3 in muscle cells. Indeed, the ER stress marker PERK was significantly higher while BiP was lower in the ME/CFS muscle samples (Fig. 5 *A* and *B*). This discordance between PERK and BiP levels in ME/CFS samples suggested impairment of the canonical ER stress pathway, termed "ER Stress Response Failure," which has been proposed to result in metabolic disorders (31). Additionally, the levels of CIV subunits (MTCO1 or CO17) showed a significant negative correlation with that of both WASF3 and PERK (Fig. 5*C*).

To further test this link between ER stress and WASF3, we treated human myoblasts with thapsigargin or tunicamycin, two well-known ER stress inducers, and observed increased WASF3 protein, but not its mRNA, in association with decreased CIV subunit MTCO1 (Fig. 5 *D*, *Left* and *SI Appendix*, Fig. S12*A*). This suggests that WASF3 is posttranslationally regulated by ER stress, and the increase in PERK and BiP confirmed the activation of ER stress in these cells by the treatments (Fig. 5 *D*, *Left*). Treating mice with another ER stress inducer lipopolysaccharide (LPS, endotoxin), which has also been used to model human chronic fatigue (33, 34), posttranscriptionally increased WASF3 levels in skeletal muscle along with the ER stress markers PERK and BiP (Fig. 5 *D*, *Right* and *SI Appendix*, Fig. S12*B*). Again, the level of WASF3 was inversely correlated with that of MTCO1, suggesting that a reduction in respiratory complex may play a role in the bioenergetic deficiency symptoms reported in humans after LPS exposure (35).

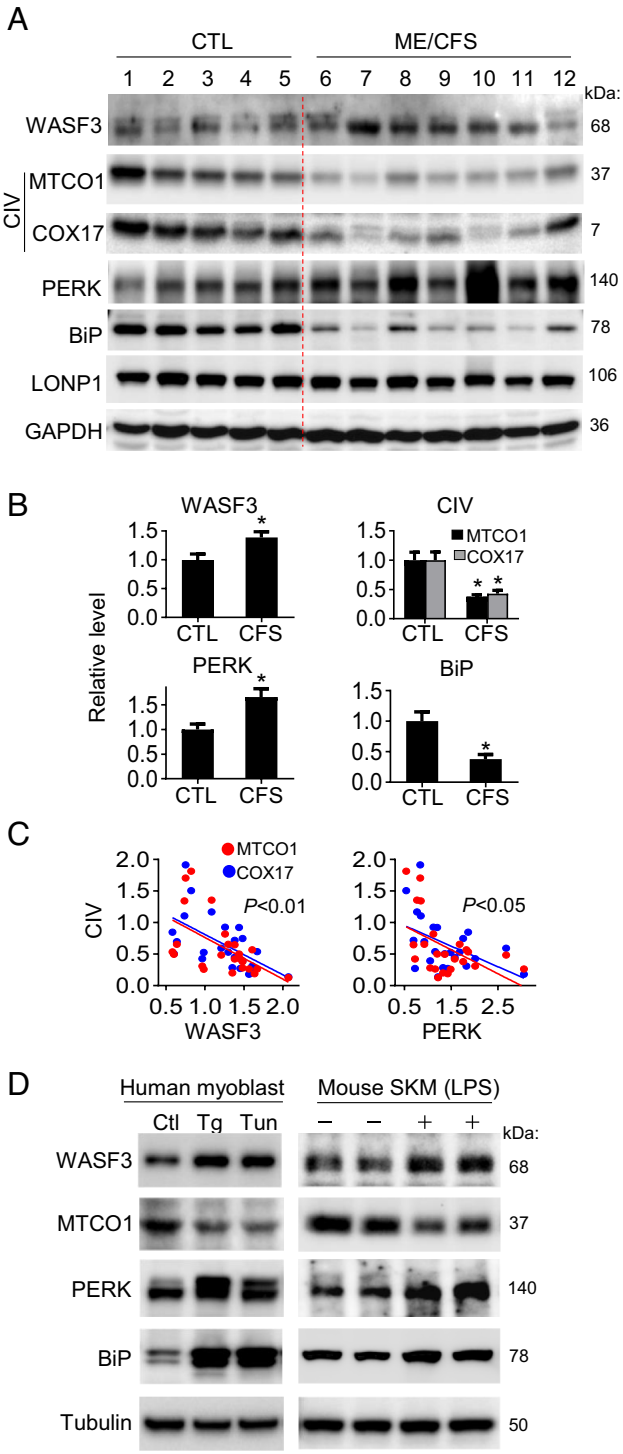

Fig. 5. WASF3 and ER stress are increased in skeletal muscle of ME/CFS patients. (*A*) Immunoblots of skeletal muscle biopsy samples from control healthy volunteers (CTL) and ME/CFS patients using the indicated antibodies. Note the reciprocal relationship between the protein levels of the CIV subunits and WASF3 or PERK. GAPDH and mitochondrial Lon peptidase 1 (LONP1) serve as protein loading controls (n = 10 to 14 from two immunoblots, see *SI Appendix*, Fig. S11). (*B*) Quantification of the indicated proteins on the immunoblots in Panel *A* and *SI Appendix*, Fig. S11. CTL (n = 10); ME/CFS (n = 14). (*C*) Correlation analyses between the protein levels of CIV subunits and WASF3 or PERK. MTCO1-WASF3, r = −0.55, *P* = 0.005; COX17-WASF3, r = −0.59, *P* = 0.003; MTCO1-PERK, r = −0.49, *P* = 0.01; COX17-PERK: r = −0.47, *P* = 0.02 (n = 24). (*D*) Immunoblot (*Left*) of human myoblasts treated with ER stress inducers tharpsigarin (Tg, 100 nM) or tunicamycin (Tun, 1 μg/mL) for 24 h. Immunoblot (*Right*) of hindlimb skeletal muscle (SKM) samples harvested from mice after treatment with another ER stress inducer lipopolysaccharide (LPS, 5 mg/kg body weight i.p.). Values are mean ± SE. Statistical difference by unpaired, two-tailed Student's *t* test. *$P < 0.05$.

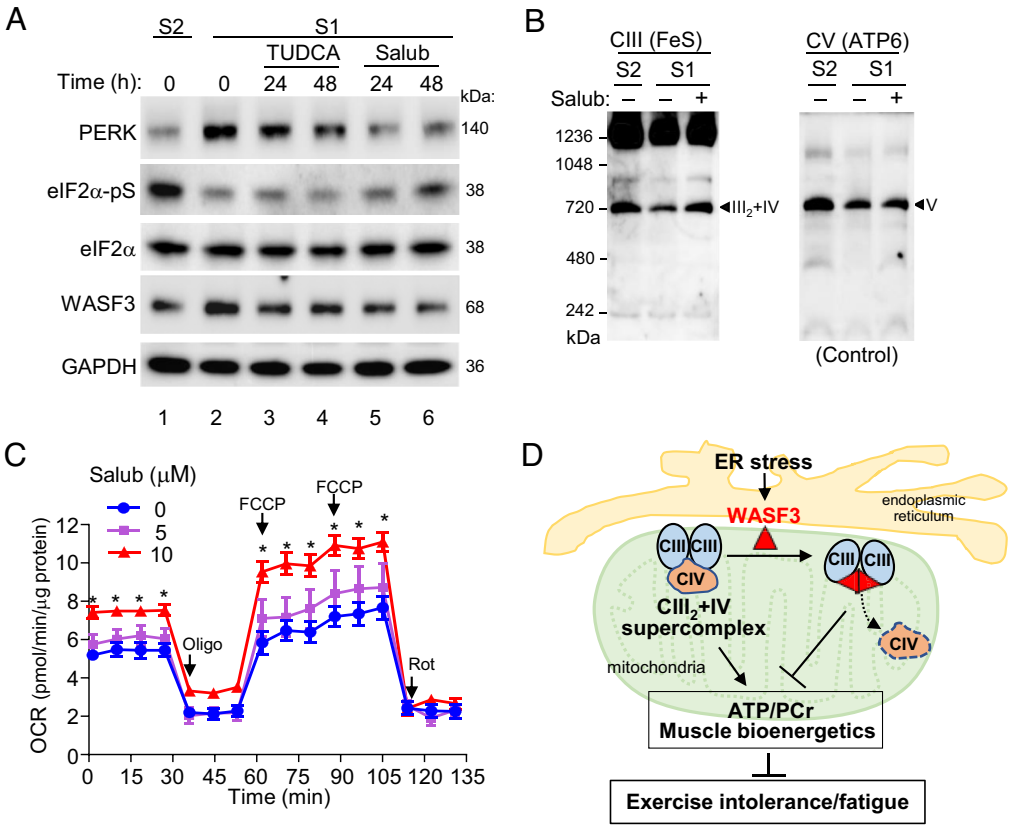

Fig. 6. Pharmacologic inhibition of ER stress improves mitochondrial respiration. (*A*) Immunoblots of patient S1 fibroblasts treated with ER stress inhibitors tauroursodeoxycholic acid (TUDCA, 100 μM) or salubrinal (Salub, 10 μM) for the indicated times. (*B*) Mitochondria purified from sibling S2 control fibroblasts and patient S1 fibroblasts with or without 10 μM salubrinal treatment for 40 h were resolved by BN-PAGE and immunoblotted with CIII Rieske FeS protein antibody. Immunoblot of ATP6 subunit of CV serves as control. (*C*) Mitochondrial oxygen consumption rate (OCR) of S1 fibroblasts treated with salubrinal for 24 h (n = 6 to 7, three experimental repeats). (*D*) A proposed model of how WASF3 regulates mitochondrial function. ER stress–induced WASF3 interacts with CIII subunits and its physical presence prevents the assembly of supercomplex III_2+IV, as demonstrated by a similar effect observed with WASF3 antibody. The disruption of mitochondrial supercomplex by WASF3 reduces oxidative phosphorylation, which could result in symptoms such as exercise intolerance and fatigue. Values are mean ± SE. Statistical difference by unpaired, two-tailed Student's *t* test. **P* < 0.05.

Pharmacologic Inhibition of ER Stress Decreases WASF3 and Rescues Supercomplex Formation and Respiration. The fibroblasts of patient S1 showed a higher basal level of PERK compared with that of her sibling S2, implying that increased ER stress may play a role in the aberrant regulation of WASF3 (Fig. 6*A*, lane 2 vs. 1). Increased ER stress would normally be expected to turn down protein translation, but intriguingly, the inhibitory phosphorylation of protein translation factor eIF2α, a target of PERK kinase activity, was unexpectedly lower (i.e., activated) in patient S1 cells (Fig. 6*A*, lane 2 vs. 1). This finding suggested that there was "ER stress response failure" in patient S1 cells as also observed in the ME/CFS muscle biopsy samples (31). We next examined the effect of reducing ER stress in S1 cells by two different inhibitors, tauroursodeoxycholic acid (TUDCA) and salubrinal (36, 37). While the effect of TUDCA was less apparent as expected of a relatively nonspecific drug, the inhibitor of protein phosphatase 1 (PP1) salubrinal, which prevents the dephosphorylation of eIF2α thereby inhibiting protein translation, was more effective in decreasing the levels of both PERK and WASF3 in S1 cells (Fig. 6*A*, lanes 3-6 vs. 2). The salubrinal treatment restored the decreased levels of SC III_2+IV in patient S1 cells, while their complex V level remained unchanged, demonstrating the targeted and specific nature of the signaling pathway (Fig. 6*B*). Finally, the recovery of supercomplex formation by salubrinal treatment resulted in a dose-dependent improvement in mitochondrial respiration of the patient S1 cells (Fig. 6*C*).

Discussion

In the current study, we have shown that WASF3, induced by ER stress, disrupts the formation of respiratory supercomplexes and reduces mitochondrial oxygen consumption, providing a molecular explanation for the energy deficiency symptoms of exercise intolerance and postexertional malaise in a patient with chronic fatigue (Fig. 6*D*). Corroborating this finding, elevated ER stress and WASF3 levels in association with reduced mitochondrial CIV subunits were observed in the skeletal muscle biopsy samples of a cohort of patients diagnosed with ME/CFS. Importantly, pharmacologic inhibition of ER stress in the cells of patient S1 decreased WASF3 expression and improved mitochondrial supercomplex formation and respiration, which may have therapeutic implications for relieving fatigue symptoms in ME/CFS.

WASF3 was initially identified as a scaffolding protein involved in cytoskeletal organization and cell motility. Although WASF3 has been linked to the mitochondria via its interaction with ATAD3A, a regulator of mitochondrial cristae structure (38), our study reveals that it can inhibit supercomplex formation by physically interacting with CIII. This molecular disruption in light of the patient's chronic fatigue symptoms is noteworthy, because genetic deficiencies of CIII have been associated with myopathy and exercise intolerance (27). Although the high expression of WASF3 in brain may be related to its actin interacting cytoskeletal function given the abundance of neuronal tubulin in this organ

(Fig. 2*E*), it could also be speculated to play a role in conferring specificity to mitochondria in neurons through its effects on supercomplex formation (39, 40). On the other hand, the dysregulation of WASF3 in neurons may disrupt mitochondrial activity, contributing to the well-described symptom of "brain fog" in ME/CFS patients (19).

It is also notable that WASF3 Tg mice express ~threefold higher levels of WASF3 in skeletal muscle compared with the ~40% increase in both the patient S1 cells and ME/CFS patient muscle biopsy samples, but interestingly the magnitude of the decreases (~30 to 50%) in MTCO1 and respiration was similar in both mouse and human samples. This observation may be due to the saturating effects of WASF3 on supercomplex regulation. The homeostasis of respiratory complex subunits can be regulated at multiple levels, such as protein translation, turnover, and stabilization by supercomplex formation. The translation of COX subunits, such as MTCO1, has been found to be coupled to the assembly of CIV and its interaction with CIII components at the early stages of supercomplex formation (41, 42). In addition, rapid degradation of newly synthesized MTCO1 also plays a role in a feedback loop that decreases MTCO1 levels upon defective complex assembly (43). Therefore, the disruption of the interaction between CIII and CIV by increased WASF3 protein could result in translational inhibition and/or degradation of the CIV core subunits, thereby decreasing their levels.

The physical and functional interactions between the ER and mitochondria are important in bioenergetic homeostasis. ER stress, especially its abnormal response by cells, has been proposed to associate with various metabolic diseases (31). ER stress normally induces the chaperone protein BiP and suppresses protein translational factor eIF2α via PERK to mitigate the unfolded protein response. However, the muscle samples of ME/CFS patients showed an opposite relationship and the cells of patient S1 also revealed loss of concordance in the levels of these ER stress proteins, implying that abnormal ER stress response may underlie the disruption in mitochondrial metabolism. Although the reason for the increased ER stress is unclear, its specific reduction in the patient's cells by salubrinal implicates the activation of eIF2α by dysregulated phosphatase PP1 as has been reported, for example, by viral infection (44). This is noteworthy because the onset of ME/CFS is often associated with viral infections by patients, and viral persistence in muscle has also been reported in some cases (45). Finally, identifying WASF3 as a direct mediator of bioenergetic deficiency raises questions about its potential role in other fatigue-associated conditions such as long COVID given that SARS-CoV-2 has been reported to persist in various tissues and could induce ER stress (11, 12, 46).

Materials and Methods

Study Participants. This study was approved by the NIH institutional review board (ClinicalTrials.gov Identifier: NCT00406445, NCT01143454), and the participants were enrolled after providing written informed consents. The patient S1 and her male sibling S2 with LFS (*TP53* P152L mutation) were screened by medical history, physical exam, and basic laboratory tests to ensure that they were in stable health. Deidentified samples of skeletal muscle from healthy volunteers and ME/CFS patients were obtained via an Intra-NIH Material Transfer Agreement (ClinicalTrials.gov NCT02669212).

Phosphorus-31 Magnetic Resonance Spectroscopy of Skeletal Muscle. An apparatus for performing submaximal foot exercise to deplete phosphocreatine (dorsiflexing the foot against 30% of the maximum weight lifted by each subject) and to measure its recovery kinetics in the tibialis anterior muscle by ^{31}P-MRS was used (14). As previously described, the tibialis anterior muscle of the supine subject was studied at 7.5 s time resolution in a 3-T MRI scanner (GE Healthcare, Waukesha, WI). A 3-inch diameter ^{31}P surface coil was placed over the tibialis anterior muscle, about one-third the distance from the origin of the tibialis anterior muscle (lateral condyle) to the medial malleolus of the dominant leg. Prior to acquisition of ^{31}P spectra, image (^{1}H)-based automatic shimming was performed to optimize the magnetic field over a region encompassing the muscle. ^{31}P spectra were continuously obtained at rest, during exercise and recovery for 3 min, 2 min, and 6 min, respectively. The spectra were acquired using a nonselective RF pulse (184-μs duration, 2,500-Hz spectral width, 2,048 data points, 1.25-s repetition time and 6 excitations) and processed with 5 Hz line broadening, zero filling, Fourier transformation, baseline correction and phase correction. PCr peak amplitudes during the recovery period were determined by fitting a model lineshape. The average PCr lineshape during 2.5 to 3.75 min of the recovery period was used as the model. PCr recovery time constant (Tc) was calculated by fitting the postexercise PCr amplitudes (7.5 s to 3.75 min, 29 data points) to a monoexponential recovery curve (47). Spectral processing and data analysis were performed using SAGE (GE Healthcare) and IDL (L3HARRIS GEOSPATIAL) software.

Cell Culture and Reagents. Patient skin biopsy samples were obtained after written informed consent as approved by the NHLBI IRB. Primary fibroblasts was prepared from the skin biopsy samples by treatment with collagenase and dispase (Invitrogen) followed by DNase (Sigma). The fibroblasts were cultured in DMEM (high glucose (4.5g/L) and GlutaMAX, Gibco 10566) supplemented with 10% fetal bovine serum and penicillin–streptomycin (50 U/mL), and the preparation of primary human myoblasts has been described previously (14). Mouse C2C12 myoblast cell line or human primary myoblast was cultured in the same DMEM medium as described above. Chemical reagents were obtained from the following sources: tunicamycin (SML1287) and thapsigargin (SML1845) from Sigma-Aldrich; tauroursodeoxycholic acid sodium (T0266) and salubrinal (SML0951) from Millipore Sigma.

Gene Knockdown and Overexpression. shRNA for the knockdown of the indicated genes were as follows: human *WASF3* (targeting sequence GCCTACTACATTGGCGCTATT, TRCN0000122939, Sigma-Aldrich); mouse p38 (*Mapk14*, MSH075380-LVRH1H, GeneCopoeia). shRNA lentiviruses were prepared using MISSION lentiviral packaging mix (Sigma-Aldrich), transduced into cells for 24 h, and drug-resistance selected for stable expression. LentiORF-WASF3 was obtained (cat# OHS6085-213583924, Dharmacon, Inc.), sequenced, and corrected according to the WASF3 reference sequence (NCBI, ENST00000361042.8). cDNAs were transfected into cells using FuGENE® HD transfection reagent (Promega).

Real-Time Reverse Transcription-PCR (RT-PCR). Real-time RT-PCR was performed as previously described using an ABI HT7900 thermal cycler (48). mRNA expression was measured by calculating the average cycle threshold (Ct) ratio relative to housekeeping gene TIF. PCR primer sequences are listed in *SI Appendix*.

Generation of WASF3 Transgenic (Tg) Mice. A human BAC clone (RP11-1089E14; ~180 kb long) was ordered from PACPAC Resources (https://bacpacresources.org/), which contains the full length human *WASF3* gene including the ~16 kb promoter region. The circular BAC DNA was linearized by digesting with PI-SceI restriction enzyme (New England Biolabs), and then microinjected into the pronuclei of zygotes collected from B6D2F1/J hybrid mice (https://www.jax.org/strain/100006). Injected zygotes were cultured overnight in KSOM medium (Millipore Sigma), and embryos reaching two-cell stage of development were implanted into the oviducts of pseudopregnant surrogate mothers (CD1 mice from Charles River Laboratory). It should be noted that the yield of WASF3-positive mice during their generation was less than expected. Offspring born to the foster mothers were genotyped by quantitative real-time PCR using the following two pairs of primers spanning approximately 10 kb of the *WASF3* gene.

Pair 1 F 5′- CTTCTGTCTTGGCATGCT -3′
R 5′- GCCATCATATTCCACTCCTGG -3′
Pair 2 F 5′- GTGGAGTACAGCGACTC -3′
R 5′- GTGGCACTTAAGTATTACACAG -3′

Mouse and Experimental Protocols. All mice were maintained and handled in accordance with the NHLBI Animal Care and Use Committee. Approximately 10-wk-old male littermates with or without WASF3 transgene were used to

determine maximal endurance capacity by treadmill testing as previously described (Columbus Instruments, OH) (49). Briefly, the mice were acclimated by running for 10 min at 10 m/min for 3 d and maximal exercise capacity were determined by graded increase in treadmill speed (10, 12, and 15 m/min for 3-5 min at each speed followed by 1.8 m/min increase every 3 min to maximal speed 28.6 m/min) on a 10% incline until all mice fell off the belt due to exhaustion. Mouse four-paw grip strength was measured by using a digital grip strength meter (Columbus Instruments, OH) (49). Tail blood lactate levels were measured using a Lactate Pro Analyzer (Arkray). Glycogen in gastrocnemius muscles was measured using a glycogen assay kit (Sigma-Aldrich) according to the manufacturer's protocol. For lipopolysaccharide (LPS) treatment experiments, wild-type C57BL/6 male mice aged 8 to 12 wk were injected with 5 mg/kg LPS i.p. and their gastrocnemius muscles were harvested for analysis.

Seahorse XF Metabolic Studies. The cells were trypsinized, resuspended in Seahorse XF DMEM assay medium (supplemented with 2 mM Glutamax, 1 mM sodium pyruvate and 25 mM glucose) (Agilent), and plated at ~5×10^4 cells/well on XF-24 well plates. The mitochondrial OCR was measured using the Agilent Seahorse XF24 Analyzer according to the manufacturer's protocol and normalized to the protein content of each well. For measuring ex vivo muscle metabolism, the whole soleus muscle was carefully dissected and embedded on islet capture microplates and its OCR and ECAR were measured.

Subcellular Fractionation of Cells and Tissues. The entire gastrocnemius muscle was dissected and placed in ice-cold PBS, and the mitochondria were isolated using standard differential centrifugation technique as described (50). Mouse C2C12 myoblasts were subcellularly fractionated as previously described (51).

Blue Native Polyacrylamide Gel Electrophoresis (BN-PAGE). Purified mitochondria were solubilized in NativePAGE sample buffer (Invitrogen) containing 1% digitonin at 4 °C for 1 h and then centrifuged at 20,000× g for 20 min. Approximately 10 μg of protein in the supernatant containing mitochondrial complexes were resolved in a 4 to 16% gradient NativePAGE Novex Bis-Tris gel, in-gel activity assayed, and immunoblotted as previously described with following modification (25). Briefly, the in-gel activity of complex I was measured by incubating the gel in solution containing NADH and nitrotetrazolium blue chloride (NTB) while the COX (complex IV) activity was detected in solution with cytochrome C and diaminobenzidine (DAB). The protein bands reacted with NTB and DAB were visualized and quantified using ChemiDoc™ Touch Imaging System (Bio-Rad). For immunoblotting, the gel after electrophoresis was incubated in transfer buffer supplemented with 2% SDS and 100 mM DTT for 15 min before being transferred to immobilon-PVDF membrane. For antibody binding of respiratory supercomplexes in vitro, 20-μg mitochondrial extract in 40 μL 1% digitonin sample buffer was incubated with 0.16-μg rabbit nonimmune IgG or the IgG against WASF3 overnight at 4 °C, the samples were then subjected to BN-PAGE analysis.

Proximity-Dependent Biotinylation Assay. Full length (1-499) or C terminus truncated (1-332) human WASF3 cDNA was cloned into the BamHI site of pCDNA3.1-BioID2-HA vector (BioFront Tech) to create a fusion with biotin ligase using the In-Fusion HD cloning kit. The fusion construct was confirmed by sequencing. C2C12 myoblasts were transiently transfected to express BioID alone or the WASF3-BioID fusion protein for 24 h in the presence of 50 μM biotin. The cells were then lysed and biotinylated proteins were isolated using Pierce Streptavidin Magnetic Beads (52).

Immunoblotting. Protein samples were solubilized in cold RIPA lysis buffer with protease inhibitor cocktail (Roche), resolved by Tris-glycine SDS PAGE, and transferred to Immobilon-P membrane (Millipore) for standard immunoblotting using ECL Plus western blotting Substrate (Pierce). The visualized proteins were quantified using ChemiDoc™ Touch Imaging System (Bio-Rad). Antibodies are listed in Supplemental Information.

Statistical Analysis.

Statistics and reproducibility. GraphPad Prism software (version 7) was used for statistical analysis. Two-tailed unpaired Student's *t* test was used for statistical comparison with corresponding controls unless otherwise noted.

Data, Materials, and Software Availability. Primary data have been deposited in FigShare (10.25444/nhlbi.23681013) (53).

ACKNOWLEDGMENTS. Research supported by the Division of Intramural Research, National Heart, Lung, and Blood Institutes (NHLBI) and National Institute of Neurological Disorders and Stroke of the NIH. We wish to thank the Li-Fraumeni syndrome family members and the many individuals associated with the ME/CFS study (ClinicalTrials.gov NCT02669212), especially Peter Jensen, who made it possible for us to obtain de-identified samples of skeletal muscle via an Intra-NIH Material Transfer Agreement. We also thank the following individuals for their important contributions: Valentina Baena Echeverri and Zulfeqhar Syed (Electron Microscopy Core, NHLBI) for EM sections of mouse skeletal muscle; Audrey Noguchi and Danielle Springer (Mutine Phenotyping Core, NHLBI) for assistance in grip force measurement of mice; Ovsanna Melikyan and Adriana Byrnes for clinical protocol administration; Yifan Zhou (Translational Stem Cell Biology Branch, NHLBI) for bioinformatics data analysis; and Dr. Michio Hirano (Columbia University Neurological Institute) for the clinical evaluation of patient S1 for mitochondrial diseases.

1. L. Bateman *et al.*, Myalgic encephalomyelitis/chronic fatigue syndrome: Essentials of diagnosis and management. *Mayo. Clin. Proc.* **96**, 2861–2878 (2021).
2. Institute of Medicine (U.S.), "Committee on the diagnostic criteria for myalgic encephalomyelitis/chronic fatigue syndrome & Institute of Medicine (U.S.). Board on the Health of Select Populations" in *Beyond Myalgic Encephalomyelitis/Chronic Fatigue Syndrome: Redefining an Illness* (The National Academies Press, Washington, D.C., 2015), p. XXI, 282 pp.
3. A. L. Komaroff, W. I. Lipkin, Insights from myalgic encephalomyelitis/chronic fatigue syndrome may help unravel the pathogenesis of postacute COVID-19 syndrome. *Trends Mol. Med.* **27**, 895–906 (2021).
4. B. D. Paul, M. D. Lemle, A. L. Komaroff, S. H. Snyder, Redox imbalance links COVID-19 and myalgic encephalomyelitis/chronic fatigue syndrome. *Proc. Natl. Acad. Sci. U.S.A.* **118**, e2024358118 (2021).
5. R. C. Vermeulen, I. W. Vermeulen van Eck, Decreased oxygen extraction during cardiopulmonary exercise test in patients with chronic fatigue syndrome. *J. Transl. Med.* **12**, 20 (2014).
6. K. Lien *et al.*, Abnormal blood lactate accumulation during repeated exercise testing in myalgic encephalomyelitis/chronic fatigue syndrome. *Physiol. Rep.* **7**, e14138 (2019).
7. J. A. Letts, L. A. Sazanov, Clarifying the supercomplex: The higher-order organization of the mitochondrial electron transport chain. *Nat. Struct. Mol. Biol.* **24**, 800–808 (2017).
8. C. Greggio *et al.*, Enhanced respiratory chain supercomplex formation in response to exercise in human skeletal muscle. *Cell Metab.* **25**, 301–311 (2017).
9. I. Ramirez-Camacho, W. R. Garcia-Nino, M. Flores-Garcia, J. Pedraza-Chaverri, C. Zazueta, Alteration of mitochondrial supercomplexes assembly in metabolic diseases. *Biochim. Biophys. Acta Mol. Basis Dis.* **1866**, 165935 (2020).
10. F. Navid, R. A. Colbert, Causes and consequences of endoplasmic reticulum stress in rheumatic disease. *Nat. Rev. Rheumatol.* **13**, 25–40 (2017).
11. T. Aoe, Pathological aspects of COVID-19 as a conformational disease and the use of pharmacological chaperones as a potential therapeutic strategy. *Front. Pharmacol.* **11**, 1095 (2020).
12. L. Rosa-Fernandes *et al.*, SARS-CoV-2 activates ER stress and Unfolded protein response. bioRxiv [Preprint] (2021). https://doi.org/10.1101/2021.06.21.449284.
13. S. C. Lewsey *et al.*, Exercise intolerance and rapid skeletal muscle energetic decline in human age-associated frailty. *JCI Insight* **5**, e141246 (2020).
14. P. Y. Wang *et al.*, Increased oxidative metabolism in the Li-Fraumeni syndrome. *N. Engl. J. Med.* **368**, 1027–1032 (2013).
15. A. Chaudhuri, P. O. Behan, In vivo magnetic resonance spectroscopy in chronic fatigue syndrome. *Prostaglandins Leukot. Essent. Fatty Acids* **71**, 181–183 (2004).
16. K. Sossey-Alaoui, T. A. Ranalli, X. Li, A. V. Bakin, J. K. Cowell, WAVE3 promotes cell motility and invasion through the regulation of MMP-1, MMP-3, and MMP-9 expression. *Exp. Cell Res.* **308**, 135–145 (2005).
17. V. Pihur, S. Datta, S. Datta, Meta analysis of Chronic Fatigue Syndrome through integration of clinical, gene expression, SNP and proteomic data. *Bioinformation* **6**, 120–124 (2011).
18. J. Wu, G. C. Wang, X. J. Chen, Z. R. Xue, Expression of WASF3 in patients with non-small cell lung cancer: Correlation with clinicopathological features and prognosis. *Oncol. Lett.* **8**, 1169–1174 (2014).
19. S. Suetsugu, H. Miki, T. Takenawa, Identification of two human WAVE/SCAR homologues as general actin regulatory molecules which associate with the Arp2/3 complex. *Biochem. Biophys. Res. Commun.* **260**, 296–302 (1999).
20. K. Sossey-Alaoui, G. Su, E. Malaj, B. Roe, J. K. Cowell, WAVE3, an actin-polymerization gene, is truncated and inactivated as a result of a constitutional t (1;13)(q21;q12) chromosome translocation in a patient with ganglioneuroblastoma. *Oncogene* **21**, 5967–5974 (2002).
21. A. Ghali *et al.*, Elevated blood lactate in resting conditions correlate with post-exertional malaise severity in patients with Myalgic encephalomyelitis/Chronic fatigue syndrome. *Sci. Rep.* **9**, 18817 (2019).
22. U. Wisloff *et al.*, Cardiovascular risk factors emerge after artificial selection for low aerobic capacity. *Science* **307**, 418–420 (2005).
23. Y. Teng *et al.*, Mitochondrial ATAD3A combines with GRP78 to regulate the WASF3 metastasis-promoting protein. *Oncogene* **35**, 333–343 (2016).
24. R. Loveless, Y. Teng, Targeting WASF3 signaling in metastatic cancer. *Int. J. Mol. Sci.* **22**, 836 (2021).
25. P. Jha, X. Wang, J. Auwerx, Analysis of mitochondrial respiratory chain supercomplexes using blue native polyacrylamide gel electrophoresis (BN-PAGE). *Curr. Protoc. Mouse Biol.* **6**, 1–14 (2016).
26. E. Fernandez-Vizarra, M. Zeviani, Mitochondrial complex III Rieske Fe-S protein processing and assembly. *Cell Cycle* **17**, 681–687 (2018).
27. M. Protasoni, M. Zeviani, Mitochondrial structure and bioenergetics in normal and disease conditions. *Int. J. Mol. Sci.* **22** (2021).

28. W. M. Behan, I. A. More, P. O. Behan, Mitochondrial abnormalities in the postviral fatigue syndrome. *Acta Neuropathol.* **83**, 61–65 (1991).
29. S. Myhill, N. E. Booth, J. McLaren-Howard, Chronic fatigue syndrome and mitochondrial dysfunction. *Int. J. Clin. Exp. Med.* **2**, 1–16 (2009).
30. B. Stussman *et al.*, Characterization of post-exertional malaise in patients with myalgic encephalomyelitis/Chronic Fatigue Syndrome. *Front. Neurol.* **11**, 1025 (2020).
31. K. R. Bhattarai, M. Chaudhary, H. R. Kim, H. J. Chae, Endoplasmic reticulum (ER) stress response failure in diseases. *Trends Cell Biol.* **30**, 672–675 (2020).
32. S. Rayavarapu, W. Coley, K. Nagaraju, Endoplasmic reticulum stress in skeletal muscle homeostasis and disease. *Curr. Rheumatol. Rep.* **14**, 238–243 (2012).
33. Z. T. Zhang *et al.*, Activation of the NLRP3 inflammasome in lipopolysaccharide-induced mouse fatigue and its relevance to chronic fatigue syndrome. *J. Neuroinflammation* **13**, 71 (2016).
34. C. G. Foster, L. M. Landowski, B. A. Sutherland, D. W. Howells, Differences in fatigue-like behavior in the lipopolysaccharide and poly I: C inflammatory animal models. *Physiol. Behav.* **232**, 113347 (2021).
35. J. Lasselin *et al.*, Fatigue and sleepiness responses to experimental inflammation and exploratory analysis of the effect of baseline inflammation in healthy humans. *Brain Behav. Immun.* **83**, 309–314 (2020).
36. Q. Xie *et al.*, Effect of tauroursodeoxycholic acid on endoplasmic reticulum stress-induced caspase-12 activation. *Hepatology* **36**, 592–601 (2002).
37. M. Boyce *et al.*, A selective inhibitor of eIF2alpha dephosphorylation protects cells from ER stress. *Science* **307**, 935–939 (2005).
38. S. Peralta *et al.*, ATAD3 controls mitochondrial cristae structure in mouse muscle, influencing mtDNA replication and cholesterol levels. *J. Cell Sci.* **131**, jcs217075 (2018).
39. D. J. Pagliarini *et al.*, A mitochondrial protein compendium elucidates complex I disease biology. *Cell* **134**, 112–123 (2008).
40. G. Pekkurnaz, X. Wang, Mitochondrial heterogeneity and homeostasis through the lens of a neuron. *Nat. Metab.* **4**, 802–812 (2022).
41. D. U. Mick *et al.*, Shy1 couples Cox1 translational regulation to cytochrome c oxidase assembly. *EMBO J.* **26**, 4347–4358 (2007).
42. A. Timon-Gomez *et al.*, Mitochondrial cytochrome c oxidase biogenesis: Recent developments. *Semin Cell Dev. Biol.* **76**, 163–178 (2018).
43. M. Bourens, A. Barrientos, A CMC1-knockout reveals translation-independent control of human mitochondrial complex IV biogenesis. *EMBO Rep.* **18**, 477–494 (2017).
44. M. Rojas, G. Vasconcelos, T. E. Dever, An eIF2alpha-binding motif in protein phosphatase 1 subunit GADD34 and its viral orthologs is required to promote dephosphorylation of eIF2alpha. *Proc. Natl. Acad. Sci. U.S.A.* **112**, E3466–E3475 (2015).
45. R. J. Lane, B. A. Soteriou, H. Zhang, L. C. Archard, Enterovirus related metabolic myopathy: A postviral fatigue syndrome. *J. Neurol. Neurosurg. Psychiatry* **74**, 1382–1386 (2003).
46. S. R. Stein *et al.*, SARS-CoV-2 infection and persistence in the human body and brain at autopsy. *Nature* **612**, 758–763 (2022).
47. Z. Argov, M. Lofberg, D. L. Arnold, Insights into muscle diseases gained by phosphorus magnetic resonance spectroscopy. *Muscle Nerve* **23**, 1316–1334 (2000).
48. W. D. Patino *et al.*, Circulating transcriptome reveals markers of atherosclerosis. *Proc. Natl. Acad. Sci. U.S.A.* **102**, 3423–3428 (2005).
49. J. Y. Park *et al.*, p53 improves aerobic exercise capacity and augments skeletal muscle mitochondrial DNA content. *Circ. Res.* **105**, 705–712 (2009).
50. C. Frezza, S. Cipolat, L. Scorrano, Organelle isolation: Functional mitochondria from mouse liver, muscle and cultured fibroblasts. *Nat. Protoc.* **2**, 287–295 (2007).
51. I. Dimauro, T. Pearson, D. Caporossi, M. J. Jackson, A simple protocol for the subcellular fractionation of skeletal muscle cells and tissue. *BMC Res. Notes* **5**, 513 (2012).
52. V. Le Sage, A. Cinti, A. J. Mouland, Proximity-dependent biotinylation for identification of interacting proteins. *Curr. Protoc. Cell Biol.* **73**, 17 (2016).
53. P. -y. Wang *et al.*, WASF3 disrupts mitochondrial respiration and may mediate exercise intolerance in myalgic encephalomyelitis/chronic fatigue syndrome. Primary data folders. FigShare. https://doi.org/10.25444/nhlbi.23681013. Deposited 13 July 2023.